1:1 Complexes of Dimethylthio- and Ethylenedithio-tetrathiafulvalenothioquinone-1,3-dithiolemethides with $CuBr_2$ as a New Type of π/d Molecular System

Masaki Iwamatsu,[†] Tsuyoshi Kominami,[†] Kazumasa Ueda,[†] Toyonari Sugimoto,*[,†] Tomohiro Adachi,[‡] Hideo Fujita,[§] Harukazu Yoshino,[||] Yoshiyuki Mizuno,[||] Keizo Murata,[||] and Motoo Shiro[⊥]

Research Institute for Advanced Science and Technology, Osaka Prefecture University, Sakai, Osaka 599-8570, Japan, Department of Chemistry, Faculty of Integrated Arts and Sciences, Osaka Prefecture University, Sakai, Osaka 599-8531, Japan, Department of Natural Environment, Faculty of Integrated Human Studies, Kyoto University, Kyoto 606-8501, Japan, Graduate School of Science, Osaka City University, Sumiyoshi, Osaka 558-8585, Japan, and Rigaku Corporation, Akishima, Tokyo 196-8666, Japan

Received February 3, 2000

The reaction of dimethylthio- (**1**) and ethylenedithio-tetrathiafulvalenothioquinone-1,3-dithiolemethides (**2**) with $CuBr_2$ gave 1:1 complexes between the donors and $CuBr_2$, **1**·$CuBr_2$ and **2**·$CuBr_2$, in which the Cu atom of $CuBr_2$ binds to the thiocarbonyl S atom in **1** and **2**. The electrical conductivity (σ) of **1**·$CuBr_2$ at room temperature was ca. 10^{-5} S cm^{-1}, while a comparatively high value of 4.0 S cm^{-1} was obtained for **2**·$CuBr_2$, whose temperature dependence of σ exhibited, however, semiconducting behavior with a very small activation energy of 0.18 eV. The observed paramagnetic susceptibilities (χ_p's) of the Cu complexes were composed of both a component due to the localized Cu spins obeying the Curie−Weiss law and a temperature-independent χ_p due to the conducting π electrons on the **1**- or **2**-stacked columns. From the Curie constants obtained, the degrees of intramolecular electron transfer from **1** and **2** to $CuBr_2$ moieties were estimated at ca. 90% and 60%, respectively. The small, negative Weiss temperatures suggest very weak antiferromagnetic interactions among the Cu spins on the $CuBr_2$ moieties.

Introduction

Much current interest is directed toward the formation of molecule-based ferromagnetic metals[1] from strong interactions between metal-conducting π electrons and localized d spins via a RKKY type of indirect exchange mechanism.[2] This kind of interaction is essentially long range and can give rise to ferromagnetic or antiferromagnetic interactions, depending on the distance between the spins. In contrast to some metals and alloys of the d and f blocks with very strong intra-atomic interaction between metal-conducting s electrons and localized d or f spins, metal-conducting π electrons and localized d spins in molecule-based materials play an important role. However, the magnitude of the π/d interaction is supposed to be very small, especially in conducting molecular materials formed by organic donors (e.g., several substituted tetrathiafulvalenes (TTF's) and tetraselenafulvalenes (TSF's)) with magnetic metal anions (MX_4 wherein M = Fe, Cu, Co, Mn; X = Cl, Br). In fact, almost all the molecular materials obtained so far exhibited very weak π/d interaction, except for special cases of (BEDT-TTF)$_3$·$CuBr_4$ (BEDT = bis(ethylenedithio)),[3] (BEDT-TTF)$_3$·$CuCl_2Br_2$,[3] λ-(BEDT-TSF)$_2$·$FeCl_4$,[4] and κ-(BEDT-TSF)$_2$·$FeBr_4$,[5] in which unusual electrical conducting and/or magnetic properties due to significant π/d interactions were observed.

Although molecular materials with strong π/d interaction might be discovered from new organic donor/magnetic metal anion systems, another approach is necessary for solving this problem more quickly. Just now, we have succeeded in the synthesis of new and unique organic donors, dimethylthio- (**1**)[6] and ethylenedithio-tetrathiafulvalenothioquinone-1,3-dithiolemethides (**2**),[7] possessing an electron-donating ability comparable to that of TTF and, furthermore, a thiocarbonyl group capable of binding to several magnetic metal salts. As a consequence, the 1:1 complexes between **1** or **2** and magnetic metal salts are expected as a new type of molecular π/d system, in which the (metal-)conducting π electrons and the localized d spins can interact with each other in a potentially more intramolecular fashion than the interionic interaction between the two components in the organic donor/magnetic metal anion

[†] Research Institute for Advanced Science and Technology, Osaka Prefecture University.
[‡] Department of Chemistry, Osaka Prefecture University.
[§] Department of Natural Environment, Kyoto University.
[||] Graduate School of Science, Osaka City University.
[⊥] Rigaku Corporation.

(1) Cassoux, P. *Science* **1996**, *272*, 1277.
(2) Elliot, J. R. In *Magnetism*; Rado, G. T., Suhl, H., Eds.; Academic Press: New York, 1965.
(3) Day, P.; Kurmoo, M.; Mallah, T.; Marsden, I. R.; Allan, M. L.; Friend, R. H.; Pratt, F. L.; Hayes, W.; Chasseau, D.; Gaultier, J.; Bravic, G.; Ducasse, L. *J. Am. Chem. Soc.* **1992**, *114*, 10722.
(4) Kobayashi, H.; Tomita, H.; Naito, T.; Kobayashi, A.; Sakai, F.; Watanabe, T.; Cassoux, P. *J. Am. Chem. Soc.* **1996**, *118*, 368.
(5) Ojima, E.; Fujiwara, H.; Kato, K.; Kobayashi, H.; Tanaka, H.; Kobayashi, A.; Tokumoto, M.; Cassoux, P. *J. Am. Chem. Soc.* **1999**, *121*, 5581.
(6) Iwamatsu, M.; Kominami, T.; Ueda, K.; Sugimoto, T.; Fujita, H.; Adachi, T. *Chem. Lett.* **1999**, 329.
(7) Iwamatsu, M.; Kominami, T.; Ueda, K.; Sugimoto, T.; Tada, T.; Nishimura, K.-i.; Adachi, T.; Fujita, H.; Guo, F.; Yokogawa, S.; Yoshino, H.; Murata, K.; Shiro, M. *J. Mater. Chem.*, submitted for publication.

10.1021/ic0001098 CCC: $19.00
Published on Web 08/04/2000

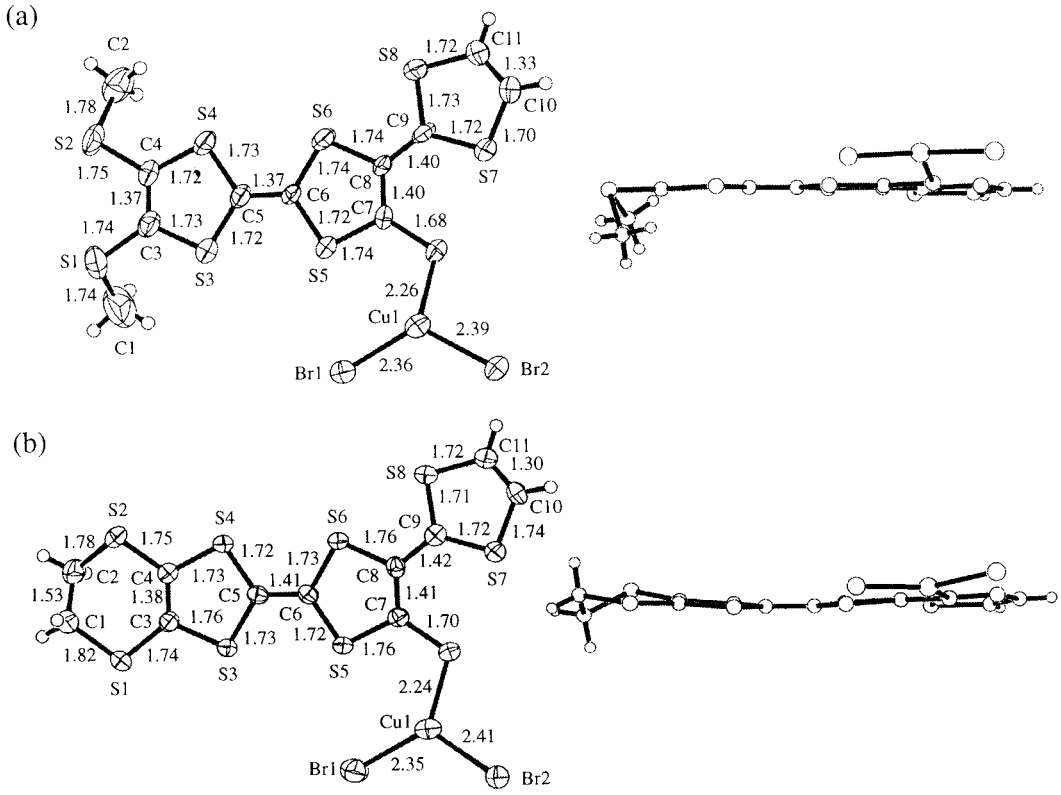

Figure 1. Molecular structures of (a) **1**·$CuBr_2$ and (b) **2**·$CuBr_2$.

salts so far. In this paper, we report on the syntheses and crystal structures of two complexes (**1**·$CuBr_2$ and **2**·$CuBr_2$) between **1** or **2** and $CuBr_2$ and also on their electrical conducting and magnetic properties.

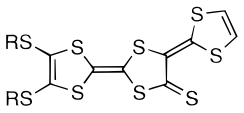

1 : R = CH_3
2 : R, R = $-CH_2CH_2-$

Experimental Section

Syntheses of 1•$CuBr_2$ and 2•$CuBr_2$. A solution of **1** or **2** (0.02 mmol) in CS_2 (3 mL) was contacted with a solution of $CuBr_2$ (0.2 mmol) in CH_3CN (3 mL) at room temperature for 1 week to afford black crystals of **1**·$CuBr_2$ (mp >300 °C) or **2**·$CuBr_2$ (mp >300 °C), quantitatively. Their elemental analyses gave satisfactory results. Calcd for **1**·$CuBr_2$ ($C_{11}H_8S_9Br_2Cu$): C, 20.26; H, 1.24. Found: C, 20.05; H, 1.34. Calcd for **2**·$CuBr_2$ ($C_{11}H_6S_9Br_2Cu$): C, 20.32; H, 0.93. Found: C, 20.48; H, 1.04.

X-ray Data Collection, Structure Solution, and Refinement. Intensity data of **1**·$CuBr_2$ and **2**·$CuBr_2$ were measured on a Rigaku AFC5R diffractometer using MoKα radiation ($\lambda = 0.71069$ Å) and a Rigaku RAXIS-IV imaging plate diffractometer with graphite monochromated MoKα radiation ($\lambda = 0.71069$ Å), respectively. Table 1 shows the crystal data and details of the data collection for **1**·$CuBr_2$ containing half a CS_2 molecule and half a H_2O molecule and for **2**·$CuBr_2$ containing one CH_3CN molecule. Intensity data were corrected for absorption with empirical methods. In the solution and refinement of these structures, the teXsan crystallographic software package was used.[8]

(8) *teXsan: Crystal Structure Analysis Package*; Molecular Structure Corporation, 1985 and 1992.

Table 1. Crystallographic Data for **1**·$CuBr_2$·$(CS_2)_{0.5}$·$(H_2O)_{0.5}$ and **2**·$CuBr_2$·CH_3CN

	1·$CuBr_2$·$(CS_2)_{0.5}$·$(H_2O)_{0.5}$	**2**·$CuBr_2$·CH_3CN
temp (K)	298	298
empirical formula	$C_{11.5}H_8O_{0.5}S_9Br_2Cu$	$C_{13}H_9NS_9Br_2Cu$
fw	698.14	691.11
cryst syst	triclinic	monoclinic
space group	$P\bar{1}$	$P2_1/c$
a (Å)	11.682(4)	7.451(1)
b (Å)	12.719(4)	24.964(3)
c (Å)	8.479(2)	11.983(2)
α (deg)	104.79(2)	90
β (deg)	106.80(2)	99.90(1)
γ (deg)	101.32(3)	90
V (Å^3)	1110.2(7)	2195.8(5)
d_{calcd} (g/cm^3)	2.088	2.090
Z	2	4
μ (cm^{-1})	5.533	5.502
tot. reflns	5422	16731
obsd reflns [$I > 2\sigma(I)$]	2256	2793
R1[a]	0.0489	0.0540
wR2[b]	0.1073	0.1474
GOF[c]	1.108	0.957

[a] $R1 = (\sum||F_o| - |F_c||)/(\sum|F_o|)$. [b] $wR2 = [\sum w(F_o^2 - F_c^2)^2/\sum w(F_o^2)^2]^{1/2}$. [c] $GOF = \{\sum[w(F_o^2 - F_c^2)^2]/(n-p)\}^{1/2}$.

The structures were solved by direct method, and refined on F_o^2 with full-matrix least-squares analysis. The hydrogen atoms were placed at calculated positions and refined according to a riding model. All non-hydrogen atoms were refined anisotropically. For **1**·$CuBr_2$·$(CS_2)_{0.5}$·$(H_2O)_{0.5}$, the final cycle of least-squares refinement on F_o^2 for 5075 data and 221 parameters converged to $wR2(F_o^2) = 0.107$ for all data and to $R1 = 0.049$ for 2256 data with $I \geq 2\sigma(I)$. For **2**·$CuBr_2$·CH_3CN, the final cycle of least-squares refinement on F_o^2 for 4986 data and 235 parameters converged to $wR2(F_o^2) = 0.147$ for all data and to $R1 = 0.054$ for 2793 data with $I \geq 2\sigma(I)$.

Electrical Conductivity, Magnetic Susceptibility, and ESR Measurements. Electrical conductivity was measured on the single crystal

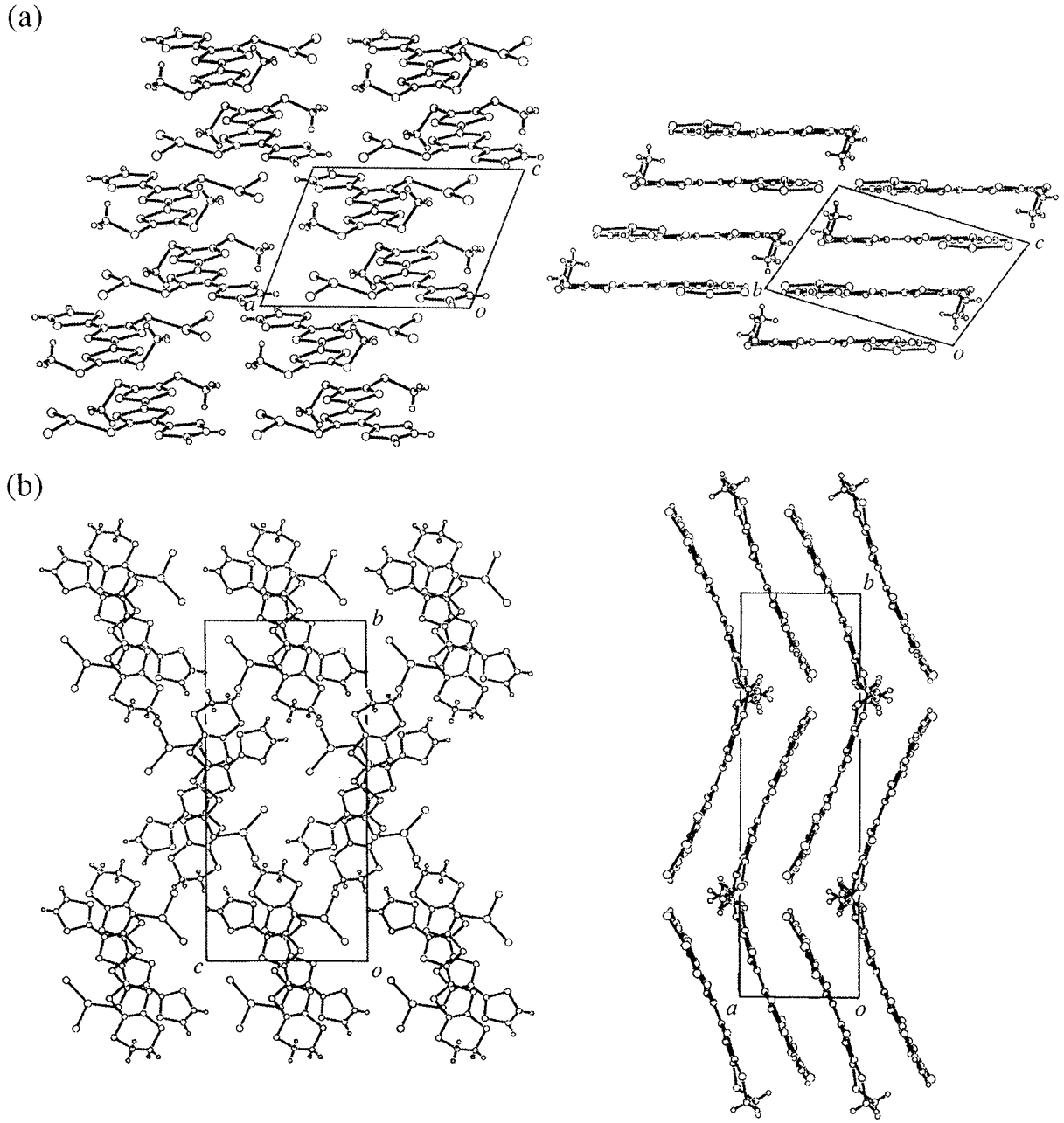

Figure 2. Projections onto the *b* and *a* axes for (a) **1**·$CuBr_2$ and the *a* and *c* axes for (b) **2**·$CuBr_2$.

of each $CuBr_2$ complex using a four-probe method in the temperature range of 180−300 K. The contact to the electrode was performed with gold paste. The magnetic susceptibility (χ_{obs}) of the microcrystals was measured between 5 and 300 K at an applied field of 1 kOe using a SQUID magnetometer (MPMS XL, Quantum Design). The paramagnetic susceptibility (χ_p) was obtained by subtracting the diamagnetic contribution calculated by a Pascal method[9] from χ_{obs}. The solid ESR spectrum was recorded using a JEOL 1X spectrometer. For determining the *g* value, a Mn^{2+}/MgO sample was used as a reference.

Results and Discussion

Molecular and Crystal Structures of 1·$CuBr_2$ and 2·$CuBr_2$. Figure 1 shows the molecular structures of both $CuBr_2$ complexes, in which the Cu atom of the $CuBr_2$ moiety is undoubtedly bound to the thiocarbonyl S atom of **1** or **2**. For **1**·$CuBr_2$, the molecular skeleton is almost planar except for two methyl groups and one $CuBr_2$ moiety, which are projected in the opposite direction with each other. The distance between the Cu atom and the thiocarbonyl S atom is 2.26 Å, which is comparable to those of several Cu−S compounds known so far.[10] The thiocarbonyl bond distance (1.68 Å) is slightly longer than that (1.66 Å) of **1**. The geometry around the Cu atom is a distorted tetrahedron. On the other hand, the whole molecular skeleton of **2**·$CuBr_2$ has high planarity. The Cu−S and thiocarbonyl bond distances are 2.24 and 1.70 Å, respectively, which are shorter and longer by 0.2 Å as compared with the corresponding values in **1**·$CuBr_2$. The geometry around the Cu atom is also a distorted tetrahedron in this $CuBr_2$ complex.

The overall top and side views of stacking structures of both $CuBr_2$ complexes are shown in Figure 2. The **1**·$CuBr_2$ and **2**·

(9) König, E. *Landolt-Bornstein, Group II: Atomic and Molecular Physics*, Vol. 2, *Magnetic Properties of Coordination and Organometallic Transition Metal Compounds*; Spring-Verlag: Berlin, 1966.

(10) Munakata, M.; Wu, L. P.; Kuroda-Sowa, T. *Adv. Inorg. Chem.* **1999**, *46*, 173.

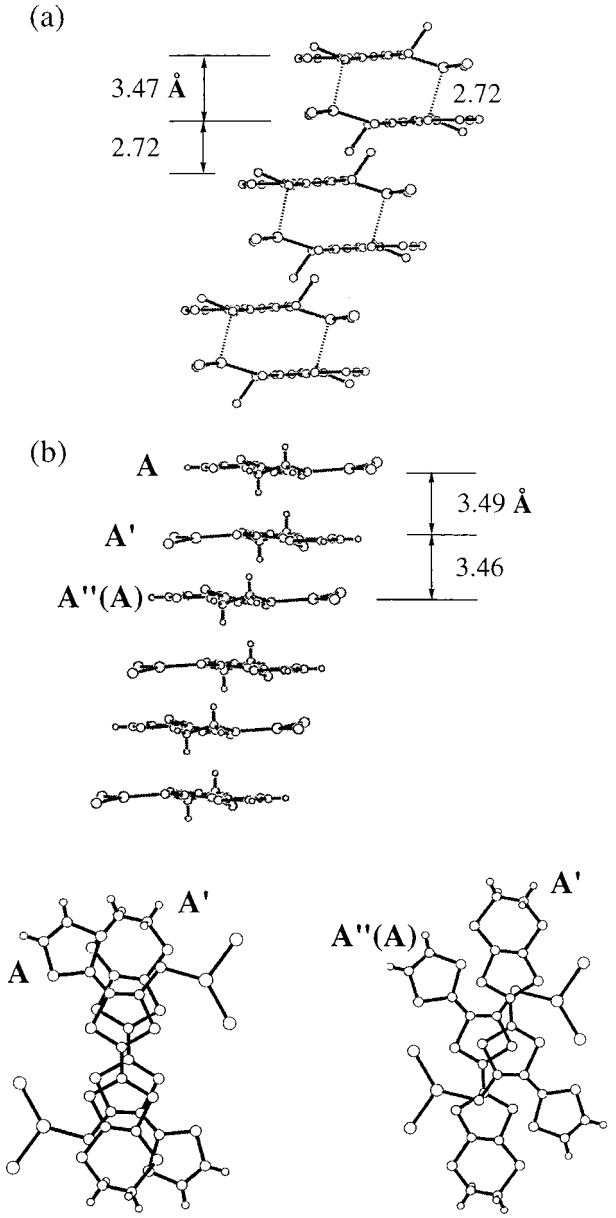

Figure 3. Stacking structures of (a) **1**·$CuBr_2$ and (b) **2**·$CuBr_2$.

$CuBr_2$ molecules are stacked along the *b* and *a* axes, respectively, to form one-dimensional columns. More detailed stacking structures of each column can be realized from Figure 3. For **1**·$CuBr_2$, two neighboring molecules form a tight dimer through close contact between the Cu atom of one molecule and one methylthio S atom of the other molecule. The corresponding intradimer Cu−S distance (2.72 Å) is fairly shorter than the sum of van der Waals radii of the Cu and S atoms (1.40 + 1.80 = 3.20 Å),[11] so the interplanar distance (d = 3.47 Å) also becomes shorter than a "π-cloud thickness" (3.50 Å).[11] The neighboring dimers have a fairly short *d* value (2.72 Å) but scarcely any effective overlap. On the other hand, the columns of **2**·$CuBr_2$ have a quasi-uniform stacking structure composed of a unit of two crystallographically independent molecules (**A**(**A**″) and **A**′), in which the contact between **A** and **A**′, albeit with a *d* value (d = 3.49 Å) very close to the π-cloud thickness, is good while **A**′ and **A**″ have inferior contact (d = 3.46 Å). As seen from Figure 4, between neighboring columns there are

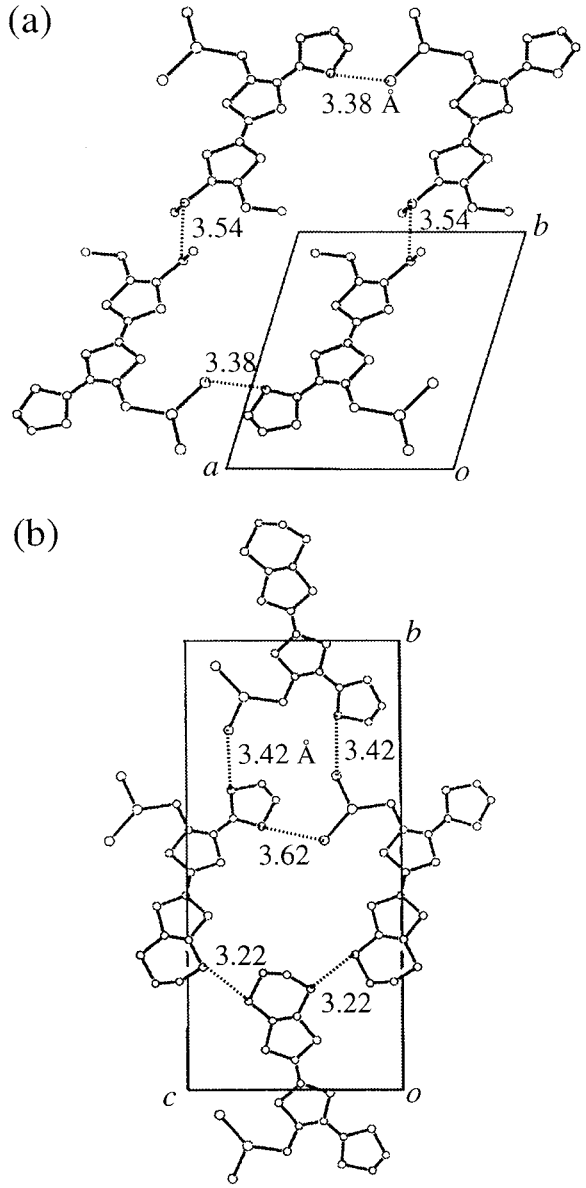

Figure 4. Contacts between columns: (a) **1**·$CuBr_2$ and (b) **2**·$CuBr_2$.

also several close contacts: between one S atom of the 1,3-dithiole ring and one Br atom of the $CuBr_2$ moiety (3.38 Å), among the methylthio S atoms (3.54 Å) of **1**·$CuBr_2$, between the S atoms of the 1,3-dithiole ring and one Br atom of the $CuBr_2$ moiety (3.42 and 3.62 Å), and among the ethylenedithio S atoms (3.22 Å) of **2**·$CuBr_2$.

Electrical Conductivities. The σ values on the single crystals of **1**·$CuBr_2$ and **2**·$CuBr_2$ at room temperature were 2.1×10^{-5} and 4.0 S cm^{-1}, respectively. The low and high electrical conducting properties of **1**·$CuBr_2$ and **2**·$CuBr_2$ can be readily recognized from the dimerized and quasi-uniform stacking structures, respectively. However, it must be also considered that the desirable degree of intramolecular electron transfer from **2** to $CuBr_2$ moieties, in producing the appropriate amount of hole carriers into the **2**-stacked columns, is responsible for the high electrical conductivity of **2**·$CuBr_2$. As will be discussed, the degrees of electron transfer were estimated at ca. 90% for **1**·$CuBr_2$ and ca. 60% for **2**·$CuBr_2$. The temperature dependence of electrical resistivity (ρ) for **2**·$CuBr_2$ showed semiconductor-like behavior with a very small activation energy of 0.18 eV, as shown in Figure 5. The semiconducting property of this $CuBr_2$ complex can be reasonably understood by considering

(11) Pauling, L. *The Nature of the Chemical Bonding*, 3rd ed.; Cornell University Press: Ithaca, NY, 1960.

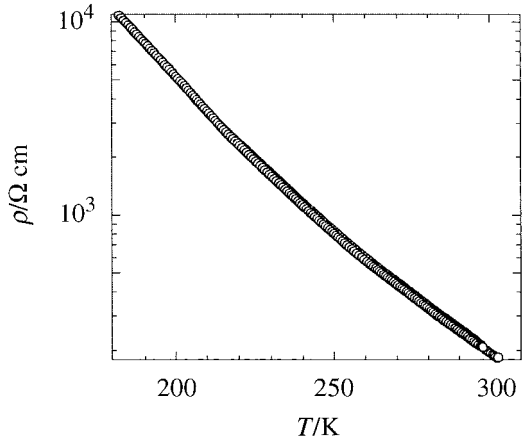

Figure 5. Temperature dependence of electrical resistivity (ρ) on the single crystal of **2**·$CuBr_2$.

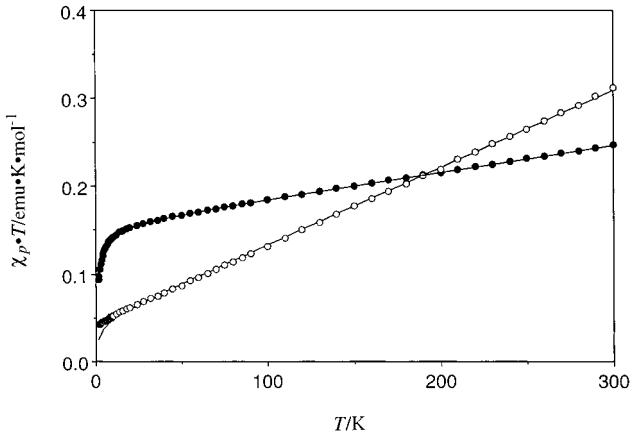

Figure 6. Temperature dependence of χ_p·T in the temperature range of 5−300 K for the microcrystals of **1**·$CuBr_2$ (○) and **2**·$CuBr_2$ (●).

that the column structure is incompletely uniform and insufficiently compact, but one cannot rule out a possibility that the localized Cu(II) ($S = {}^1/_2$) d spins on the $CuBr_2$ moieties have influence on the destabilization of the metallic state even at high temperatures.

Magnetic Susceptibilities. The temperature dependence of χ_p was investigated in the temperature range of 5−300 K for the two $CuBr_2$ complexes. Figure 6 shows the χ_p·T vs T plots. For both cases, the χ_p obtained was well interpreted as the sum of a component obeying the Curie−Weiss law ($C/(T - \theta)$, where C is the Curie constant and θ the Weiss temperature) and a temperature-independent component (χ_π). The best fitting between experimenal and theoretical data gave $C = 0.045$ emu·K·mol^{-1}, $\theta = -1.9$ K, and $\chi_\pi = 8.8 \times 10^{-4}$ emu·mol^{-1} for **1**·$CuBr_2$ and $C = 0.16$ emu·K·mol^{-1}, $\theta = -1.2$ K, and $\chi_\pi = 3.1 \times 10^{-4}$ emu·mol^{-1} for **2**·$CuBr_2$. From the crystal structures of these complexes, it is most reasonable to assume that the component obeying the Curie−Weiss law is due to the localized Cu(II) d spins on the $CuBr_2$ moieties, while the χ_π component is associated with the spins of conducting π electrons on the **1**- or **2**-stacked columns. When the electron transfer occurs from **1** or **2** to $CuBr_2$ moieties, the Cu atom of each $CuBr_2$ moiety becomes an intermediate state of Cu(I) ($S = 0$) and Cu(II). Of course, with an increasing degree of electron transfer, the ratio of Cu(I)/Cu(II) increases, and the spin amount on the Cu atom decreases. On the other hand, **1** or **2** is in part converted to the corresponding radical cation to produce hole carriers on the **1**- or **2**-stacked columns. Since the hole carriers exhibit semiconducting behavior in this case, the χ_π corresponds to an almost temperature-independent χ_p in the low-temperature region of the χ_pT plot obtained by strong antiferromagnetically interacting spin systems.[12−14] When the physical meanings of C, θ, and χ_π are taken into account, the magnetic properties of the two $CuBr_2$ complexes can be readily understood. Thus, from the C value for **1**·$CuBr_2$, the spin amount on the Cu atom of each $CuBr_2$ moiety is equal to 12% of the value (0.38 emu·K·mol^{-1}) calculated as a Cu(II) spin entity, which corresponds to an electron transfer of 88% from **1** to $CuBr_2$ moieties. Furthermore, a very small and negative θ value suggests weak antiferromagnetic interaction between the remaining spins on the Cu atoms. On the other hand, for **2**·$CuBr_2$, the degree of electron transfer from **2** to $CuBr_2$ moieties is 58%, a value smaller than that for **1**·$CuBr_2$. A very weak antiferromagnetic interaction between the Cu d spins also occurs in this case.

ESR Spectra. The magnetic susceptibility results of **1**·$CuBr_2$ and **2**·$CuBr_2$ can be understood in more detail from their solid ESR measurements. For **1**·$CuBr_2$, one weak doublet signal with $g = 2.0069$ was observed at 298 K, and the spectral shape and g value were not changed at 77 K, although there was a marked increase in intensity. Since the g value is very close to that ($g = 2.0070$) of the radical cation BF_4 salt of **1**,[15] this signal can be reasonably considered to be due to the spins of conducting π electrons on the **1**-stacked columns. A signal due to the d spin, albeit very small, on the Cu atom of each $CuBr_2$ moiety should be observed. However, this supposedly low-intensity signal may be hidden by the comparatively much stronger π signal. In contrast, the spectrum of **2**·$CuBr_2$ was composed of two different kinds of signals at 298 and 77 K. One doublet signal appeared at $g = 2.0066$, which can also be assigned to the spins of conducting π electrons on the **2**-stacked columns. The other two signals, $g_\parallel = 2.0918$ and $g_\perp = 2.2370$ at 77 K with the averaged g value at 298 K, are obviously due to the d spins on the Cu atoms of $CuBr_2$ moieties. The appearance of these signals in **2**·$CuBr_2$ was made possible by much a larger d spin than in **1**·$CuBr_2$.

Concluding Remarks

As is obvious from the present results, **1** and **2** indeed served as electron donors capable of binding to one molecule of $CuBr_2$, which can act as an oxidizing agent for **1** and **2** and also as a localized d spin source. Accordingly, new Cu complexes, such as **1**·$CuBr_2$ and **2**·$CuBr_2$, can continue to be expected as a new type of molecular π/d system, although unfortunately, both metal-like electrical conductivity and spin ordering of localized Cu d spins on the $CuBr_2$ moieties from strong interactions with the conducting π electrons on the **1**- or **2**-stacked columns were not realized by these $CuBr_2$ complexes. Presumably, the main cause of the lack of achievement of the above properties is the incompletely uniform and/or insufficiently compact stacking structures of **1**·$CuBr_2$ and **2**·$CuBr_2$, since adequate intramolecular electron transfer from **2** to $CuBr_2$ moieties in producing holes exhibits metallic behavior in the case of **2**·$CuBr_2$. If this was actually the case, the expected metal-like conductivity/ferromagnetism might be achieved by applying high pressure to **1**·$CuBr_2$ and **2**·$CuBr_2$. At present, we are carrying out these experiments. Furthermore, we are searching for new $CuBr_2$

(12) Ogawa, M. Y.; Hoffman, B. M.; Lee, S.; Yudkowsky, M.; Halperin, W. P. *Phys. Rev. Lett.* **1986**, *57*, 1177.
(13) Yakushi, K.; Yamakado, H.; Ida, T.; Ugawa, A. *Solid State Commun.* **1991**, *78*, 919.
(14) Ueda, K.; Goto, M.; Iwamatsu, M.; Sugimoto, T.; Endo, S.; Toyota, N.; Yamamoto, K.; Fujita, H. *J. Mater. Chem.* **1998**, *8*, 2195.
(15) Iwamatsu, M.; Ueda, K.; Sugimoto, T.; Fujita, H. Unpublished results.

complexes with derivatives other than **1** and **2** which can exhibit the above properties under a normal pressure condition.

Acknowledgment. This work was supported by a grant-in-aid for scientific research on priority areas (B) (1224209) from the Ministry of Education, Science and Culture, Japan.

Supporting Information Available: Tables listing detailed crystallographic data, atomic positional parameters, and bond lengths and angles for **1**·$CuBr_2$ and **2**·$CuBr_2$ and microcrystal ESR spectra of **1**·$CuBr_2$ and **2**·$CuBr_2$ at 298 and 77 K. This material is available free of charge via the Internet at http://pubs.acs.org.

IC0001098